PHYSICAL REVIEW D **92,** 095001 (2015)

Radiative linear seesaw model, dark matter, and $U(1)_{B-L}$

Weijian Wang[1,*] and Zhi-Long Han[2,†]

[1]*Department of Physics, North China Electric Power University, Baoding 071003, China*
[2]*School of Physics, Nankai University, Tianjin 300071, China*

(Received 11 August 2015; published 2 November 2015)

In this paper we propose a radiated linear seesaw model where the naturally small term μ_L is generated at the one-loop level and its soft breaking of lepton number symmetry contributes to the spontaneous breaking (SSB) of $B-L$ gauge symmetry. The value of $B-L$ charges for new particles are assigned to satisfy the cancellation of anomalies. It is found that some new particles may have exotic values of $B-L$ charge such that there exists residual $Z_2 \times Z_2'$ symmetry even after SSB of $B-L$ gauge symmetry. The $Z_2 \times Z_2'$ discrete symmetry stabilizes these particles as dark matter candidates. In the model, two classes of inert fermions and scalars with different $B-L$ charges are introduced, leading to two-component dark matter candidates. The lepton-flavor-violation processes, the relic density of dark matter, the direct detection of dark matter and the phenomenology at the LHC are investigated.

DOI: 10.1103/PhysRevD.92.095001 PACS numbers: 14.60.Pq, 12.60.Fr, 95.35.+d

I. INTRODUCTION

The origin of tiny but nonzero neutrino masses observed by neutrino oscillation experiments [1] remains so far a mystery, and so provides us with an opportunity to search for new physics beyond the standard model (SM). Perhaps the simplest scenario which may explain the neutrino puzzle is to introduce the Majorana mass that breaks the global $B-L$ symmetry though the dimension-five Weinberg operator $\lambda LL\Phi\Phi/\Lambda$ [2]. This effective operator can be realized though various pathways which depend on the new physics scales the associated heavy intermediate state(s) lie at. For instance in the case of the widely known type-I seesaw mechanism [3] with right-handed Majorana ingredients N_R as massages, one needs the super-heavy masses for N_R i.e. 10^{14-16} GeV to fit the observed sub-eV neutrino mass. The right-handed neutrinos are too heavy to be detected at future experiments. In contrast, in the so-called low-scale scenarios, the small neutrino mass is not only due to the massage state with heavy mass but also to another naturally small mass parameter which breaks the lepton number symmetry. This is the basic idea behind many schemes including the type-II seesaw model [4], inverse seesaw model [5] and linear seesaw model [6,7]. In these models, the mass of massage particles can be lowered down to a TeV or even hundreds of GeV, a scale to be explored at collider experiments.

On the other hand, the Planck data has shown that 26% of the energy density of our Universe is occupied by dark matter (DM). In the view of particle physics, the weakly interacting massive particles (WIMPs) are the most promising dark matter candidates. In recent years, a class of models were proposed to incorporate the neutrino mass puzzle and the existence of dark matter in a unified framework. In these models, the neutrino masses are generated at loop level and the dark matter is naturally contained as an inert particle, where the Z_2 symmetry or a $U(1)_X$ symmetry is used to guarantee the stability of dark matter. The radiated generation of neutrino mass has been realized at the one-loop level [8–10], two-loop level [11–15] and three-loop level [16]. The systematic analysis of one- and two-loop realizations for possible topologies was performed in Ref. [17].

In this paper, we propose a radiated linear seesaw model where the lepton number violation is due to the spontaneous symmetry breaking (SSB) of $U(1)_{B-L}$ gauge symmetry, while the naturally small mass parameter is generated at the one-loop level. The linear seesaw model was fist studied in the left-right theory with the gauge group $SU(3) \times SU(2)_L \times SU(2)_R \times U(1)_{B-L}$ [6], and subsequently inspired by $SO(10)$ theory in the presence of gauge singlets [7]. In the linear seesaw scenario, Ψ_R and Ψ_L are added to the SM so that the Lagrangian is given by

$$L = M_D \bar{\nu}_L \Psi_R + M_\Psi \bar{\Psi}_R \Psi_L + \mu_L \tilde{\nu}_L \Psi_L + \text{H.c.} \quad (1)$$

The neutrino mass matrix in the basis of $(\nu_L,\ \Psi_R^c,\ \Psi_L)$ is

$$M_\nu = \begin{pmatrix} 0 & M_D & \mu_L \\ M_D^T & 0 & M_\Psi \\ \mu_L^T & M_\Psi^T & 0 \end{pmatrix}. \quad (2)$$

The light neutrino mass is given by $m_\nu \sim \mu_L M_D M_\Psi^{-1}$. Note that the μ_L violates the lepton number symmetry and plays the role of a naturally small parameter. Thus it seems natural that there exists a suppression mechanism where the μ_L term is generated via a loop diagram while the

*wjnwang96@aliyun.com
†hanzhilong@mail.nankai.edu.cn

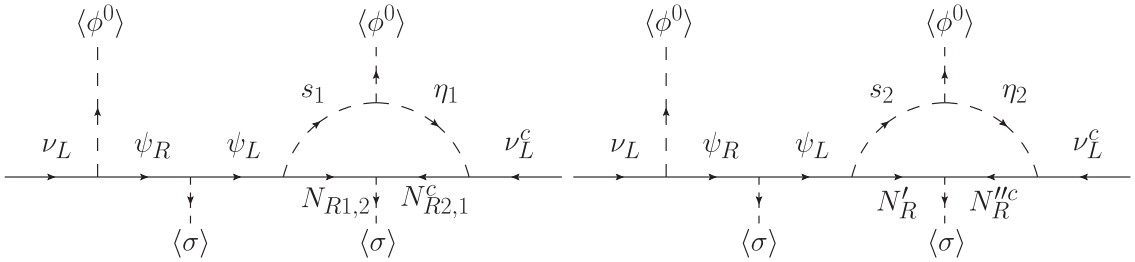

FIG. 1. The one-loop diagrams for neutrino masses in our model.

soft-breaking of lepton number symmetry may contribute to the SSB of $B-L$ gauge symmetry. Moreover, when the WIMPs as the dark matter candidates are involved in the loop diagram, we can reasonably assume they are generated by a vacuum expectation value (VEV) with respect to the SSB of $B-L$ gauge symmetry at the TeV scale. These are the main motivations of this work.

Following the spirit of Ref. [14], the value of $B-L$ charges should be carefully assigned since the cancellation of anomalies must be satisfied. It is found that some new particles may have exotic values of $B-L$ charge such that there exists residual $Z_2\times Z_2'$ symmetry even after SSB of $B-L$ gauge symmetry. The $Z_2\times Z_2'$ discrete symmetry stabilizes these particles from decaying to SM ingredients. Thus the lightest particle with the same exotic value of $B-L$ charge can be a dark matter candidate. In practice, we introduce two classes of inert fermions and scalars to realize the model, leading to two-component dark matter candidates.

The existence of new fermions and scalars provides rich phenomena. Tiny neutrino masses are explained with a one-loop-induced linear-seesaw-like mechanism. The charged scalar mediates lepton flavor violation (LFV) of charged leptons. The relic density and the direct detection of the two-component dark matter are investigated. The properties of the discovered SM Higgs will be changed by the new particles. And these new particles provide plenty of new signatures at the LHC. In particular, multilepton signals with missing transverse energy $\not{E}_T$ can be used to test our model. We find that our model can satisfy current constraints from the phenomena mentioned above.

The rest of paper is organized as follows. In Sec. II, we introduce the realization of the radiative linear seesaw and multicomponent dark matter from gauged $U(1)_{B-L}$. In Sec. III, we discuss the phenomena of lepton flavor violation, dark matter and collider signatures. Conclusions are given in Sec. IV.

II. MODEL

A. Model setup

In our model the neutrino masses are generated via the diagram depicted in Fig. 1. The new particle content and their charge assignments are listed in Table. I. We add N_Ψ generation Weyl fermions Ψ_{Ri}, Ψ_{Li}, N_1 right-handed Majorana neutrinos $N_{R\alpha}$, and N_2 pairs of right-handed Majorana neutrinos N_R' and N_R'' to the SM where i, α and β are the generation indices. All the new fermions are singlets under the SM gauge group. Five new scalars η_1, s_2, η_2, s_2 and σ are also added to the SM. Because the new fermions are all SM singlets, the $B-L$ gauge symmetry satisfies all anomaly cancellations except for $[U(1)_{B-L}]\times[\text{Gravity}]^2$ and $[U(1)_{B-L}]^3$ [18]. Considering the conditions for the absence of the $[U(1)_{B-L}]\times[\text{Gravity}]^2$ and $[U(1)_{B-L}]^3$ anomaly, one has

$$3+\left(-\frac{1}{2}\right)N_1+xN_2+(-1-x)N_2+(-1)N_\psi=0, \quad (3)$$

$$3+\left(-\frac{1}{2}\right)^3N_1+x^3N_2+(-1-x)^3N_2+(-1)^3N_\psi=0. \quad (4)$$

After solving the anomaly-free condition, one obtains

$$N_1=2,\quad N_2=1,\quad N_\psi=1,\quad x=\frac{\sqrt{2}-1}{2}. \quad (5)$$

Thus we have the some inert particles classified into two parts. In the first class, there are two Majorana right-handed neutrinos (N_{R1}, N_{R2}) and the inert scalars (η_1, s_1) with their $B-L$ charge being $-\frac{1}{2}$. In the second class, we obtain a pair of Majorana right-handed neutrinos (N_R', N_R'') along with the inert scalars (η_2, s_2) whose $B-L$ charges are irrational numbers ($\frac{\sqrt{2}-1}{2}$ or $\frac{-\sqrt{2}-1}{2}$). One notices that the new particles with both $-\frac{1}{2}$ and the irrational numbers cannot decay into SM particles. Therefore the lightest particles belonging to the same class are stable and can be regarded as a dark matter

TABLE I. New particle content: $G_{\text{SM}}\times U(1)_{B-L}$.

Particles	Ψ_R	Ψ_L	N_R	N_R'	N_R''	η_1	s_1	η_2	s_2	σ
$SU(2)_L$	1	1	1	1	1	2	1	2	1	1
$U(1)_Y$	0	0	0	0	0	$\frac{1}{2}$	0	$\frac{1}{2}$	0	0
$U(1)_{B-L}$	-1	0	$-\frac{1}{2}$	x	$-1-x$	$-\frac{1}{2}$	$-\frac{1}{2}$	x	x	1

candidate. The relevant Lagrangian for the Yukawa sector is given by

$$\begin{aligned}-L_Y &= y_l\overline{L_l}\psi_R i\tau_2\Phi^* + y'\overline{\psi_L}\psi_R\sigma + h_\alpha\overline{N_{R\alpha}}\psi_L s_1 \\ &+ f_{\alpha l}\overline{L_l^c}N^c_{R\alpha}i\tau_2\eta_1^* + \frac{1}{2}Y_\alpha\overline{N^c_{R\alpha}}N_{R\alpha}\sigma \\ &+ h\overline{N'_R}\psi_L s_2 + f_l\overline{L_l^c}N''^c_R i\tau_2\eta_2^* + \frac{1}{2}Y\overline{N''^c_R}N'_R\sigma + \text{H.c.}\end{aligned} \tag{6}$$

Without losing generality, we work in the basis where the mass term of $N_{R1,2}$ is diagonal. As for the mass term of N'_R and N''_R, one can redefine the fields as

$$\chi_1 = \frac{1}{\sqrt{2}}(N'_R + N''_R), \qquad \chi_2 = \frac{i}{\sqrt{2}}(N'_R - N''_R) \tag{7}$$

so that

$$\frac{1}{2}Y\overline{N''^c_R}N'_R\sigma \to \frac{1}{2}Y(\overline{\chi_1^c}\chi_1 + \overline{\chi_2^c}\chi_2)\sigma. \tag{8}$$

Now we get two Majorana neutrino eigenstates having the same masses. Note that there is no interplay between the Yukawa terms of $N_{R1,2}$ and (N'_R, N''_R) because of the $B-L$ charge assignments they have.

The scalar potential in our model is given by

$$\begin{aligned}V(\Phi,\sigma,\eta_1,s_1,\eta_2,s_2) &= -\mu_\Phi^2\Phi^\dagger\Phi + \lambda_\Phi(\Phi^\dagger\Phi)^2 - \mu_\sigma^2|\sigma|^2 + \lambda_\sigma|\sigma|^4 \\ &+ \mu_{\eta_1}^2\eta_1^\dagger\eta_1 + \lambda_{\eta_1}(\eta_1^\dagger\eta_1)^2 + \mu_{\eta_2}^2\eta_2^\dagger\eta_2 + \lambda_{\eta_2}(\eta_2^\dagger\eta_2)^2 \\ &+ \mu_{s_1}^2|s_1|^2 + \lambda_{s_1}|s_1|^4 + \mu_{s_2}^2|s_2|^2 + \lambda_{s_2}|s_2|^4 + \lambda_{s_1s_2}|s_1|^2|s_2|^2 \\ &+ \lambda_{\eta_1\Phi}(\Phi^\dagger\Phi)(\eta_1^\dagger\eta_1) + \lambda'_{\eta_1\Phi}(\eta_1^\dagger\Phi)(\Phi^\dagger\eta_1) + \lambda_{\eta_2\Phi}(\Phi^\dagger\Phi)(\eta_2^\dagger\eta_2) + \lambda'_{\eta_2\Phi}(\eta_2^\dagger\Phi)(\Phi^\dagger\eta_2) \\ &+ \lambda_{\eta_1\eta_2}(\eta_1^\dagger\eta_1)(\eta_2^\dagger\eta_2) + \lambda'_{\eta_1\eta_2}(\eta_1^\dagger\eta_2)(\eta_2^\dagger\eta_1) \\ &+ \lambda_{s_1\Phi}|s_1|^2(\Phi^\dagger\Phi) + \lambda_{s_1\eta_1}|s_1|^2(\eta_1^\dagger\eta_1) + \lambda_{s_1\eta_2}|s_1|^2(\eta_2^\dagger\eta_2) \\ &+ \lambda_{s_2\Phi}|s_2|^2(\Phi^\dagger\Phi) + \lambda_{s_2\eta_1}|s_2|^2(\eta_1^\dagger\eta_1) + \lambda_{s_2\eta_2}|s_2|^2(\eta_2^\dagger\eta_2) \\ &+ \lambda_{\sigma\Phi}|\sigma|^2(\Phi^\dagger\Phi) + \lambda_{\sigma\eta_1}|\sigma|^2(\eta_1^\dagger\eta_1) + \lambda_{\sigma\eta_2}|\sigma|^2(\eta_2^\dagger\eta_2) \\ &+ \lambda_{s_1\sigma}|s_1|^2|\sigma|^2 + \lambda_{s_2\sigma}|s_2|^2|\sigma|^2 + (\mu_1 s_1^\dagger\Phi^\dagger\eta_1 + \mu_2 s_2^\dagger\Phi^\dagger\eta_2 + \text{H.c.})\end{aligned} \tag{9}$$

where the values of μ_Φ^2, μ_σ^2, $\mu_{\eta_1}^2$, $\mu_{\eta_2}^2$, $\mu_{s_1}^2$ and $\mu_{s_2}^2$ are taken as positive and the values of the coupling constants μ_1 and μ_2 in trilinear terms can be set as positive by rephasing s_1 and s_2. Notice that there are no terms like $s_1\sigma^2$ or $s_2\sigma^2$ appearing in the scalar potential. This has two meanings. First, the inert scalars $\eta_{1,2}$ and $s_{1,2}$ do not acquire a VEV after the SSB of Φ and σ. Second, there exists a residual $Z_2 \times Z_2'$ symmetry under which all the inert particles are odd even after the breakdown of $B-L$ symmetry. Therefore the residual $Z_2 \times Z_2'$ symmetry stabilizes the inert particles, making them the two-component dark matter candidates.

B. Matrices of scalar particles

After the SSB, the scalars Φ and σ are parametrized as

$$\Phi = \begin{pmatrix} G^+ \\ \frac{v_\phi+\phi_0+iG_\phi}{\sqrt{2}} \end{pmatrix}, \qquad \sigma = \frac{v_\sigma+\sigma_0+iG_\sigma}{\sqrt{2}} \tag{10}$$

where $v_\phi \simeq 246$ GeV is the VEV of the SM Higgs doublet scalar and v_σ is responsible for the SSB of $B-L$ symmetry [19]. The Nambu-Goldstone bosons G^+, G_ϕ and G_σ are absorbed by the longitudinal components of the W, Z and Z' gauge bosons. For simplicity, we ignore the kinetic mixing between the $U(1)_Y$ and $U(1)_{B-L}$ gauge bosons [20]. Therefor the VEV v_σ provides a mass for the $U(1)_{B-L}$ gauge boson Z' as $M_{Z'} = g_{B-L}v_\sigma$, where g_{B-L} is the $U(1)_{B-L}$ gauge coupling constant. For the extra gauge boson Z', LEP-II provides a combined bound $M_{Z'}/g_{B-L} > 7$ TeV [21], which is just the lower bound on v_σ. Then we obtain the mass matrix for the CP-even scalars ϕ_0 and σ_0

$$\begin{aligned}M^2(\phi_0,\sigma_0) &= \begin{pmatrix} \cos\theta & \sin\theta \\ -\sin\theta & \cos\theta \end{pmatrix}\begin{pmatrix} M_h^2 & 0 \\ 0 & M_H^2 \end{pmatrix} \\ &\times \begin{pmatrix} \cos\theta & -\sin\theta \\ \sin\theta & \cos\theta \end{pmatrix}\end{aligned} \tag{11}$$

where h stands for the SM-like Higgs [22,23] and H is an extra CP-even Higgs boson [24–26] whose masses respectively are

$$M_h^2 = \lambda_\Phi v_\phi^2 + \lambda_\sigma v_\sigma^2 - \sqrt{(\lambda v_\phi^2 - \lambda_\sigma v_\sigma^2)^2 + \lambda_{\sigma\Phi}^2 v_\phi^2 v_\sigma^2}, \tag{12}$$

$$M_H^2 = \lambda_\Phi v_\phi^2 + \lambda_\sigma v_\sigma^2 + \sqrt{(\lambda v_\phi^2 - \lambda_\sigma v_\sigma^2)^2 + \lambda_{\sigma\Phi}^2 v_\phi^2 v_\sigma^2} \tag{13}$$

and the mixing angle θ is determined as

$$\sin 2\theta = \frac{2\lambda_{\sigma\Phi} v_\phi v_\sigma}{M_H^2 - M_h^2}. \tag{14}$$

On the other hand, the inert scalars (η_1, s_1) and (η_2, s_2) do not mix with Φ and σ due to the residual Z_2 symmetry. The mass matrix for the inert scalar fields are

$$M(\eta_1, s_1, \eta_2, s_2) = (\eta_1^\dagger, s_1^\dagger, \eta_2^\dagger, s_2^\dagger) \times \begin{pmatrix} M_{11} & M_{12} & 0 & 0 \\ M_{21} & M_{22} & 0 & 0 \\ 0 & 0 & M_{33} & M_{34} \\ 0 & 0 & M_{43} & M_{44} \end{pmatrix} \begin{pmatrix} \eta_1 \\ s_1 \\ \eta_2 \\ s_2 \end{pmatrix} \tag{15}$$

where

$$\begin{aligned} M_{11} &= \mu_{\eta_1}^2 + \frac{1}{2}\lambda_{\phi\eta_1} v_\phi^2 + \frac{1}{2}\lambda'_{\phi\eta_1} v_\phi^2 + \frac{1}{2}\lambda^2_{\sigma\eta_1} v_\sigma^2, \\ M_{22} &= \mu_{s_1}^2 + \frac{1}{2}\lambda_{s_1\phi} v_\phi^2 + \frac{1}{2}\lambda_{s_1\sigma} v_\sigma^2, \\ M_{33} &= \mu_{\eta_2}^2 + \frac{1}{2}\lambda_{\phi\eta_2} v_\phi^2 + \frac{1}{2}\lambda'_{\phi\eta_2} v_\phi^2 + \frac{1}{2}\lambda^2_{\sigma\eta_2} v_\sigma^2, \\ M_{44} &= \mu_{s_2}^2 + \frac{1}{2}\lambda_{s_2\phi} v_\phi^2 + \frac{1}{2}\lambda_{s_2\sigma} v_\sigma^2, \\ M_{12} &= M_{21} = \frac{\mu_1}{\sqrt{2}} v_\phi, \\ M_{34} &= M_{43} = \frac{\mu_2}{\sqrt{2}} v_\phi. \end{aligned} \tag{16}$$

There is also no mixing between (η_1, s_1) and (η_2, s_2), and therefore a residual Z_2' symmetry between the two classes can be realized. After diagonalizing the mass matrix, we obtain the mass eigenstates of the inert scalars as

$$\begin{pmatrix} A_{1,2}^0 \\ H_{1,2}^0 \end{pmatrix} = \begin{pmatrix} \cos\theta_{1,2} & -\sin\theta_{1,2} \\ \sin\theta_{1,2} & \cos\theta_{1,2} \end{pmatrix} \begin{pmatrix} \eta_{1,2}^0 \\ s_{1,2}^0 \end{pmatrix},$$

$$\sin 2\theta_{1,2} = \frac{\sqrt{2}\mu_{1,2} v_\phi}{M_{A_{1,2}}^2 - M_{H_{1,2}}^2} \tag{17}$$

where

$$M_{A_{1,2}}^2 = \frac{1}{2}(M_{\eta_{1,2}}^2 + M_{s_{1,2}}^2 + \sqrt{(M_{\eta_{1,2}}^2 - M_{s_{1,2}}^2)^2 + 2\mu_{1,2}^2 v_\phi^2}), \tag{18}$$

$$M_{H_{1,2}}^2 = \frac{1}{2}(M_{\eta_{1,2}}^2 + M_{s_{1,2}}^2 - \sqrt{(M_{\eta_{1,2}}^2 - M_{s_{1,2}}^2)^2 + 2\mu_{1,2}^2 v_\phi^2}). \tag{19}$$

Here $M_{\eta_1} \equiv M_{11}$, $M_{s_1} \equiv M_{22}$, $M_{\eta_2} \equiv M_{33}$ and $M_{s_2} \equiv M_{44}$.

C. Neutrino mass

As shown in Fig. 1, the tiny neutrino masses are generated by the linear seesaw mechanism except that the μ_L terms are induced by a one-loop diagram. The effective mass matrix for the active neutrinos depicted in Fig. 1 is expressed as

$$M_{\nu ll'} = M^I_{\nu ll'} + M^{II}_{\nu ll'} \tag{20}$$

where

$$\begin{aligned} M^I_{\nu ll'} &= \frac{v_\phi \sin\theta_1 \cos\theta_1}{16\pi^2\sqrt{2}M_\psi} y_l \sum_{i=1}^{2} h_i f_{il'} M_i \left[\frac{M_{A_1^2}}{M_i^2 - M_{A_1}^2}\ln\left(\frac{M_{A_1}^2}{M_i^2}\right) - \frac{M_{H_1^2}}{M_i^2 - M_{H_1}^2}\ln\left(\frac{M_{H_1}^2}{M_i^2}\right)\right] + (l \leftrightarrow l'), \\ M^{II}_{\nu ll'} &= \frac{v_\phi \sin\theta_2 \cos\theta_2}{16\pi^2\sqrt{2}M_\psi} y_l h f_{l'} M_\chi \left[\frac{M_{A_2^2}}{M_\chi^2 - M_{A_2}^2}\ln\left(\frac{M_{A_2}^2}{M_\chi^2}\right) - \frac{M_{H_2}^2}{M_\chi^2 - M_{H_2}^2}\ln\left(\frac{M_{H_2}^2}{M_\chi^2}\right)\right] + (l \leftrightarrow l') \end{aligned} \tag{21}$$

where $M_i (i = 1, 2)$ denotes the masses for N_{R1} and N_{R2}; M_χ denotes the masses for the eigenstates of N'_R and N''_R. Tiny neutrino masses can be obtained using the following benchmark points:

$$\begin{aligned} &\mu_1 = \mu_2 = 0.1\ \text{GeV}, \quad y = h = 0.0028, \quad f = 0.01, \quad M_\psi = 300\ \text{GeV}, \\ &M_{N_{R1}} = 149.5\ \text{GeV}, \quad M_{N_{R2}} = 200\ \text{GeV}, \quad M_\chi = 150\ \text{GeV}, \\ &M_{A_1^0} = 300\ \text{GeV}, \quad M_{\eta_1^\pm} = 270\ \text{GeV}, \quad M_{H_1^0} = 1000\ \text{GeV}, \\ &M_{A_2^0} = 700\ \text{GeV}, \quad M_{\eta_2^\pm} = 690\ \text{GeV}, \quad M_{H_2^0} = 62\ \text{GeV} \end{aligned} \tag{22}$$

with the index of the Yukawa couplings suppressed for simplicity. Then we get $M_\nu = 0.0164\ \text{eV}(\approx\sqrt{\Delta m_{13}^2})$.

The benchmark point given above seems unreasonable since the M_ν becomes a rank-1 matrix as

$$M_\nu \sim D \equiv \begin{pmatrix} 1 & 1 & 1 \\ 1 & 1 & 1 \\ 1 & 1 & 1 \end{pmatrix} \tag{23}$$

which is obviously not consistent with the results of neutrino oscillation experiments. However, one recalls that the expression of the matrix (23) is just the so-called flavor democratic model studied by many authors and related to some flavor symmetries [27]. The matrix D can be diagonalized as

$$V_\nu^T D V_\nu = \begin{pmatrix} 0 & 0 & 0 \\ 0 & 0 & 0 \\ 0 & 0 & 3 \end{pmatrix} \equiv \hat{D},$$
$$V_\nu = \frac{1}{\sqrt{6}} \begin{pmatrix} \sqrt{3} & 1 & \sqrt{2} \\ -\sqrt{3} & 1 & \sqrt{2} \\ 0 & -2 & \sqrt{2} \end{pmatrix}. \tag{24}$$

The unitary matrix V_ν corresponds to the democratic mixing pattern. Since $\hat{D}$ contains a dominant nonzero element at the (3,3) position, the flavor democratic structure in M_ν in Eq. (23) can be viewed as a good approximation for the rank-2 neutrino mass matrix exhibiting the strong hierarchal feature for the normal order of the neutrino mass spectrum i.e. $m_1 = 0 \ll m_2 = \sqrt{\Delta m^2_{12}} \ll m_3 = \sqrt{\Delta m^2_{13}}$. It is noted that the democratic mixing matrix V_ν itself is not consistent with the Pontecorvo-Maki-Nakagawa-Sakata (PMNS) matrix $U_{\rm PMNS}$ measured by experiments; however if one recalls the formula $U_{\rm PMNS} = V_l^\dagger V_\nu$ then the V_ν can be corrected by the charged-lepton sector to fit the neutrino oscillation data [28]. The flavor symmetry realization of the mixing angle is beyond the scope of this work and we will not discuss any further details on this topic.

The small values of $\mu_{1,2}$ lead to $\sin 2\theta_{1,2} = (3.8, 7.2) \times 10^{-5}$, which plays a key role in the suppression of tiny neutrino masses. The choice of values of $\mu_{1,2}$ is mainly for phenomenological consideration. First, in the case of scalar DM, there exists the $Z - S - S^*$ coupling proportional to $\sin^2\theta_{1,2}$. The spin-independent elastic cross section of DM requires $\sin\theta_{1,2} < 0.05$ [29], setting an upper limit on $\mu_{1,2} \sim (10\ \text{GeV})$ for electroweak (EW)-scale inert scalars. Second, given the benchmark point that assumes the inert particles at the EW-scale and Yukawa couplings of order 10^{-2} or 10^{-3}, one expects rich phenomena of new physics for the LHC and LFV processes. We emphasize that larger values of $\mu_{1,2}$ are possible if the values of the Yukawa couplings are decreased. But this predicts too small branching ratios for LFV processes. The decreased Yukawa couplings are also hardly detected on collider machine. Furthermore a Yukawa coupling that is too small also seems unnatural from the viewpoint of model building. Another solution is to increase the mass of ψ or an inert particle to the TeV scale, which is beyond the reach of the LHC. For the DM candidate $N_{R1}(H_2^0)$, its mass is set to be about half of the mass of the s-channel mediator $H(\text{h})$. Then one obtains a large enough DM annihilation cross section to account for the relic density. For the heavy dirac fermion ψ and inert doublet scalars η_1, A_0^1, we choose their masses around 300 GeV, so that they are testable at the LHC. The other inert scalars are around the TeV scale and suppress the value of the neutrino mass.

III. PHENOMENOLOGY

A. Lepton flavor violation

The Yukawa interactions of the charged scalar $\eta^\pm$ will contribute to the LFV processes of charged leptons. Detail studies on LFV processes in scotogenic models [9] have been carried out in Refs. [30,31]. Currently, the most severe constraint comes from the MEG Collaboration on muon radiative decay with an upper limit $\text{BR}(\mu \to e\gamma) < 5.7 \times 10^{-13}$ (90% C.L.) [32]. In our model, the analytical branching ratio of $\mu \to e\gamma$ is calculated as [30,33]

$$\text{BR}(\mu \to e\gamma) = \frac{3\alpha_{em}}{64\pi G_F^2} \left| \sum_{i=1}^{2} \frac{f_{i\mu} f_{ie}^*}{M^2_{\eta_1^+}} F\left(\frac{M^2_{N_i}}{M^2_{\eta_1^+}}\right) + \frac{f_l f_l^*}{M^2_{\eta_2^+}} F\left(\frac{M^2_\chi}{M^2_{\eta_2^+}}\right) \right|^2, \tag{25}$$

where the loop function $F(x)$ is

$$F(x) = \frac{1 - 6x + 3x^2 + 2x^3 - 6x^2 \ln x}{6(1-x)^4}. \tag{26}$$

The benchmark point in Eq. (22) predicts $\text{BR}(\mu \to e\gamma) = 9.8 \times 10^{-14}$, which satisfies the current limit and is in the reach of future sensitivity [34]. The limits on τ observables are less stringent [35,36]. With the natural Yukawa structure at our benchmark point, the predicted $\text{BR}(\tau \to \mu\gamma) = 5.8 \times 10^{-13}$ is far beyond the future sensitivity. But on the other hand, a hierarchal Yukawa structure $|f_{ie}| \lesssim |f_{i\mu}| \lesssim |f_{i\tau}|$ with $f_{i\tau} \sim \mathcal{O}(1)$ is still allowed from the phenomenological point of view. In this case, fermionic dark matter candidate F annihilation in the mass region between 2 GeV and 3 TeV through the t-channel exchange of η can satisfy the dark matter relic density bound [31]. And as a consequence of the hierarchal Yukawa structure, dark matter F annihilates mainly into third-family leptons: $\tau^+\tau^-$ and $\nu_\tau\bar{\nu}_\tau$.

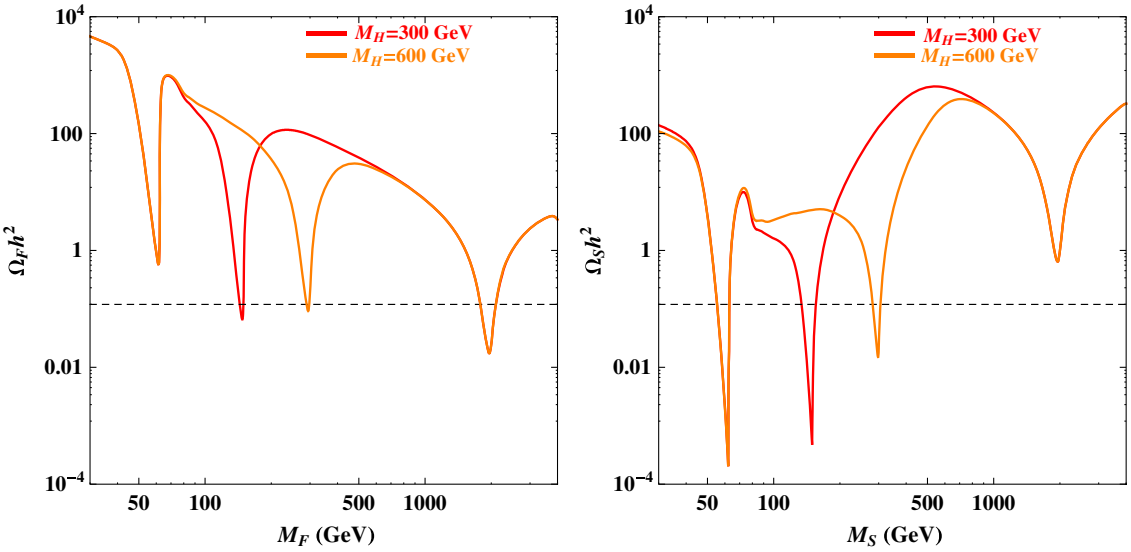

FIG. 2 (color online). Relic density of fermion (left) and scalar (right) dark matter as a function of $M_{\rm DM}$ for one dark matter candidate. Here, we set the relevant scalar interaction coupling $\lambda_{\eta_2\Phi} = \lambda'_{\eta_2\Phi} = \lambda_{s_2\Phi} = -0.001$, $\lambda_{\sigma\eta_2} = \lambda_{s_2\sigma} = -0.001$. We also fix $M_h = 125$ GeV, $M_H = 300/600$ GeV, $\sin\theta = 0.3$, $M_{Z'} = 4$ TeV, and $v_\sigma = 8$ TeV.

B. Dark matter

In our model, a multicomponent dark matter scenario is possible due to the residual Z_2' symmetry between two sets of new scalars and fermions. For instance, we choose the lightest fermion N_{R1} (referred to as F) in set one and the lightest scalar H_2^0 (referred to as S) in set two as dark matter candidates. These dark matter candidates must satisfy two experimental constrains: 1) the dark matter relic density observed by Plank [37] $\Omega_{\rm DM}h^2 = 0.1193 \pm 0.0014$; 2) the cross section for the direct detection of dark matter scattering off of a nucleon set by LUX [29].

The theoretical calculation of the dark matter relic density is well described in Ref. [38], and it is calculated with the help of the packages FEYNRULES [39] and micrOMEGAs [40] in our analysis. Because the t-channel Yukawa portal may suffer constraints from LFV or neutrino masses, and at our benchmark point, the t-channel contribution to the relic density is less than 1%, we will focus on the s-channel $h/H/Z'$ portal for simplicity. First, the relic density of fermion/scalar dark matter for one dark matter candidate is presented in Fig. 2, where we neglect the conversion $F\bar{F} \leftrightarrow SS^*$ between the two dark matter candidates. For the fermion dark matter F, the light h portal can not acquire a sufficient annihilation cross section, while the heavy H portal is still promising when $M_F \sim M_H/2$, which is due to the suppression of the large $v_\sigma = 8$ TeV. Anyway, the Z' portal can easily satisfy the relic density

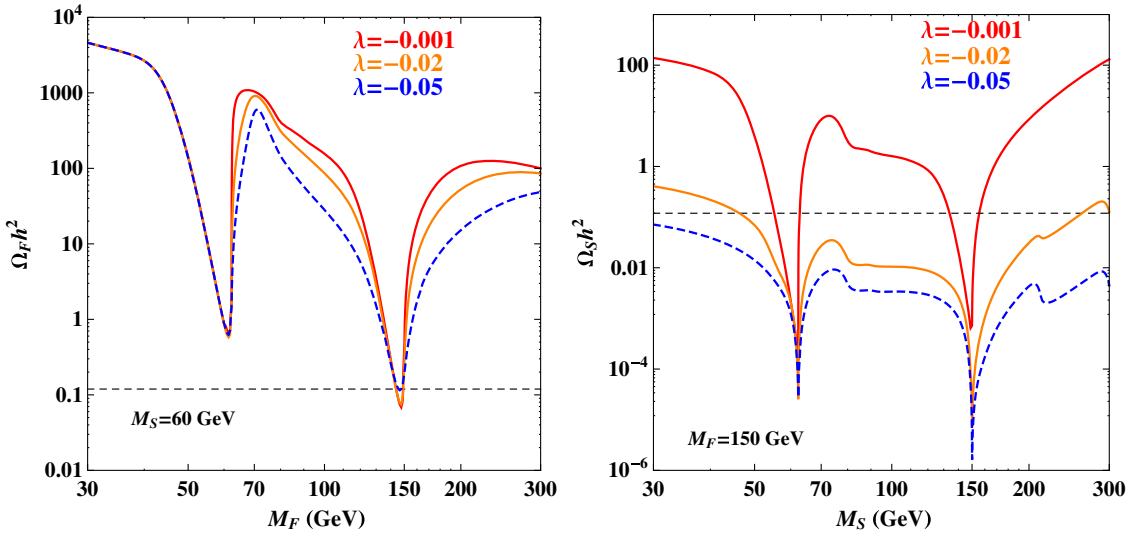

FIG. 3 (color online). The dependence of the F/S relic density on λ.

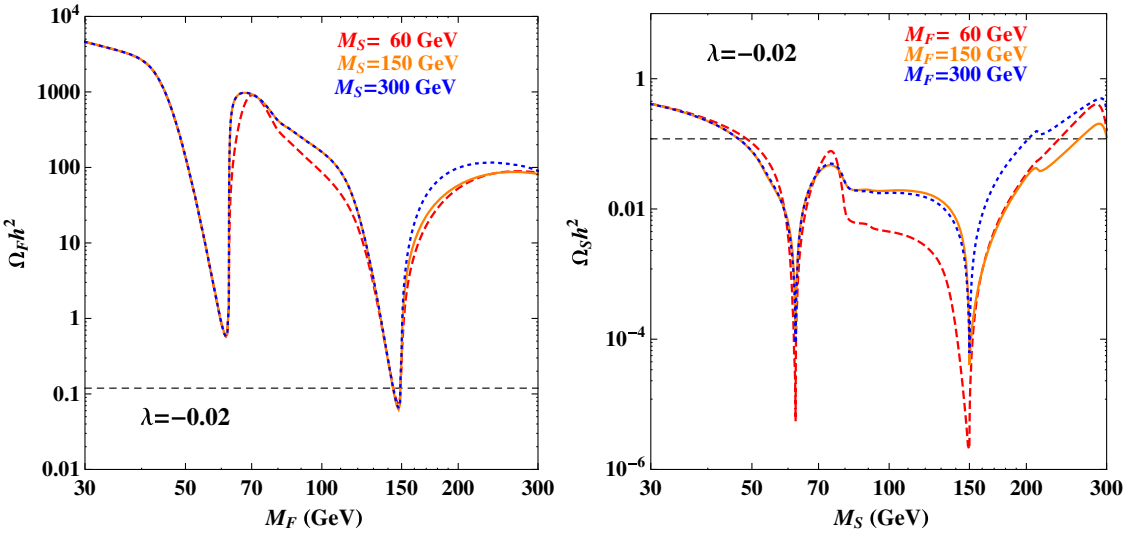

FIG. 4 (color online). The effect of two-component dark matter conversion on the F/S relic density for fixed $\lambda = -0.02$.

when $M_F \sim M_{Z'}/2$. For the scalar dark matter S, it is predominantly made from the singlet scalar s_2^0, due to the small mixing θ_2. The relic density can easily be attained when $M_S \sim M_h/2$ and $M_S \sim M_H/2$, while the Z' portal is not promising, mainly due to the small $B-L$ charge of S and the suppression of the heavy $M_{Z'}$.

Second, we take into account the conversion of two-component dark matter $F\bar{F} \leftrightarrow SS^*$, which can be mediated by the s-channel $h/H/Z'$, where the H portal is expected to be the dominant one. Therefore, HSS^* and $HF\bar{F}$ are the two most relevant couplings for studying conversion. For simplicity, we further assume $\lambda_{\sigma\eta_2} = \lambda_{s_2\sigma} = \lambda$, which determines the HSS^* coupling, and fix the other parameters as shown in Fig. 2 if not mentioned otherwise.

The dependence of the F/S relic density on λ is shown in Fig. 3. For the fermion dark matter, when $M_F > M_S$, a larger λ gives a larger $F\bar{F} \leftrightarrow SS^*$ annihilation rate, and therefore a smaller the relic density. It is clear that the $\Omega_F h^2$ can differ by about 1 order of magnitude between $\lambda = -0.001$ and $\lambda = -0.05$. But when $M_F < M_S$, the effect of the conversion $F\bar{F} \to SS^*$ is quite small. We notice that for $\lambda = -0.05$, the $H \to SS^*$ can greatly enhance the total decay width of H, which causes an increase of $\Omega_F h^2$ around $M_F \sim M_H/2$. For the scalar dark matter, an increase of λ will decrease the relic density significantly due to the increase of SS^* annihilation. But, the friction of the conversion $SS^* \to F\bar{F}$ stays the same, since the Yukawa coupling $HF\bar{F}$ is fixed by M_F. The arguments are true if we exchange the roles of F and S, and fix the HSS^* coupling while verifying the $HF\bar{F}$ coupling.

Another aspect of conversion is the masses of the two dark matter candidates. The left (right) panel of Fig. 4 shows the $F(S)$ relic density for $M_{S(F)} = 60, 150, 300$ GeV with $\lambda = -0.02$. In the case of fermion dark matter, it is clear that the smaller the M_S the larger the $F\bar{F} \to SS^*$ annihilation rate, and therefore the smaller the relic density. For a relatively heavy $M_S = 150, 300$ GeV, the conversion has a tiny effect on the F relic density when $M_F < M_H/2$. In the case of scalar dark matter, the dependence of $\Omega_S h^2$ on M_F is a little complicated, since the $HF\bar{F}$ coupling is directly related to the M_F. For $M_S < 80$ GeV, the effect of conversion is relatively small, and one expects that the larger the M_F the smaller the S relic density, which is mainly caused by the increase of the $HF\bar{F}$ coupling. In the medium-mass region $80 < M_S < 200$ GeV, the conversion effect would be dominant, and thus the smaller the M_F the smaller the S relic density. In the high-mass region, the conversion effect is comparable to the $HF\bar{F}$ coupling effect, which makes the dependence of $\Omega_S h^2$ on M_F nonlinear. In a word, the HSS^* and $HF\bar{F}$ couplings play a vital role in dark matter conversion. The conversion can take place in both directions $F\bar{F} \to SS^*$ and $SS^* \to F\bar{F}$ when $M_F \sim M_S$, which can be obtained when both F and S are mainly annihilated through the H portal. If this is not the case, only the conversion of the heavier one into the light one is relevant [41].

Finally, we discuss the constraints from the direct detection of dark matter. The current experimental constraints assume the existence of only one dark matter species. However two-component dark matter candidates are predicted in our model. Therefore the contribution of the cross section on the nucleon for each species should be rescaled by the fraction factor of the relic density. We define the fraction of the mass density of the ith dark matter in the case of multicomponent dark matter as [42,43]

$$\epsilon_i = \frac{\Omega_i h^2}{\Omega_{\rm CDM} h^2}, \tag{27}$$

where $i = F, S$ in our consideration. Therefore, the upper limit of direct detection is

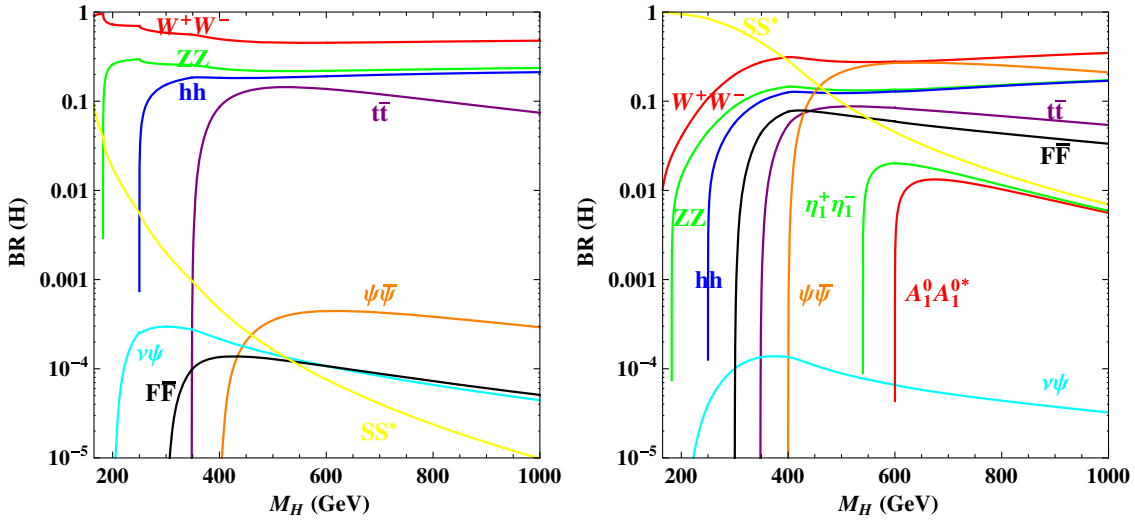

FIG. 5 (color online). Branching ratios of H as a function of M_H for $\sin\theta = 0.3$ (left) and $\sin\theta = 0.01$ (right) at our benchmark point in Eq. (22).

$$\frac{\epsilon_F}{M_F}\sigma_{F-N} + \frac{\epsilon_S}{M_S}\sigma_{S-N} < \frac{\sigma_{\rm exp}}{M_{\rm DM}}. \quad (28)$$

Here, $\sigma_{F-N}(\sigma_{S-N})$ denotes the scattering cross section of $F(S)$ with a nucleon N. The benchmark point in Eq. (22) gives the spin-independent scattering cross section $\sigma^{SI}_{F-N} = 1.10\times10^{-46}$ cm^2 ($\sigma^{SI}_{S-N} = 1.62\times10^{-44}$ cm^2) with $\Omega_F h^2 = 1.12\times10^{-1}$ ($\Omega_S h^2 = 2.64\times10^{-4}$). Although the bare σ^{SI}_{S-N} is larger than the LUX upper constraint 1.1×10^{-47} cm^2/GeV [29], the contribution of the scalar S to the scattering on the nucleon is suppressed because of its small fraction $\epsilon_S = 2.21\times10^{-3}$. The value of the expression on left side of Eq. (28) is 1.3×10^{-48} cm^2/GeV, which is smaller than the current LUX bound. Thus, the fermion dark matter is dominant in this scenario, while the scalar dark matter must be less than 4% to escape the current LUX bound.

C. Collider signatures

As shown at our benchmark point [Eq. (22)], the new particles are all at the electroweak scale, which makes them testable at the LHC. Interactions between these new particles and the SM Higgs h will of course modify the properties of h, and thus give us some indirect hints. Nowadays the most precise measurement of M_h is the combined results of ATLAS and CMS [44]:

$$M_h = 125.09 \pm 0.21({\rm stat}) \pm 0.11({\rm sys})\ {\rm GeV}. \quad (29)$$

Apparently, the extra new scalars and fermions would change the decay rates of the SM Higgs h. For instance, mixing between h and the additional scalar singlet H will modify tree-level h decays. And the additional charged scalars $\eta^{\pm}_{1,2}$ will contribute to the loop-induced decays as $h\to\gamma\gamma$ [45].

It is well known that, for Higgs-portal dark matter, upper limits on the Higgs invisible decay are also interpreted as upper limits on the dark matter-nucleon scattering cross section [46]. Direct measurement of Higgs invisible decay in association with Z by ATLAS set an upper limit of 75% at 95% C.L. [47]. The combined analysis with the Higgs signal strength gives a more tight upper limit of 37% at 95% C.L. [48–50]. In the future, the weak boson fusion channel might have the ability to probe invisible decay to 2–3% with 3000 fb^{-1} at the LHC [51]. Light dark matter candidates in our model will contribute the invisible decays of h in our model. In the case of scalar dark matter, the branching ratio of Higgs invisible decay, i.e., BR$(h\to SS^*)$ is 1.7% for $M_S = 62$ GeV with $\lambda_{s_2\Phi} = \lambda_{s_2\sigma} = -0.001$, $\sin\theta = 0.3$. On the other hand for fermion dark matter, BR$(h\to F\bar{F})$ is 1.7×10^{-6} for $M_F = 62$ GeV with $v_\sigma = 8$ TeV, $\sin\theta = 0.3$, although it might not be favored by the constraints on the relic density of dark matter.

Then we discuss the mixing between h and H. The analysis of the signal strength of h constrains $\sin^2\theta < 0.23$ at 95% C.L. [52,53]. The direct search for H in the ZZ and WW channels now has pushed this limit down to $\sin^2\theta < 0.1$ with no new physics contribution to the decays of H [54]. Future hadron colliders, i.e., HL-LHC, have the ability to probe $\sin^2\theta \sim 4\times10^{-2}$, and lepton colliders, i.e., CEPC, could reach $\sin^2\theta \sim 2\times10^{-3}$ [55]. In Fig. 5, we show the branching ratios of H for two values of $\sin\theta(0.3, 0.01)$. For a relatively large mixing angle $\sin\theta = 0.3$, the heavy neutral Higgs H decays predominantly into SM particles. The branching ratio of invisible decay $H\to SS^*$ can reach 10% for $M_H \sim 165$ GeV, and we expect that it becomes dominant when $M_H < 160$ GeV.

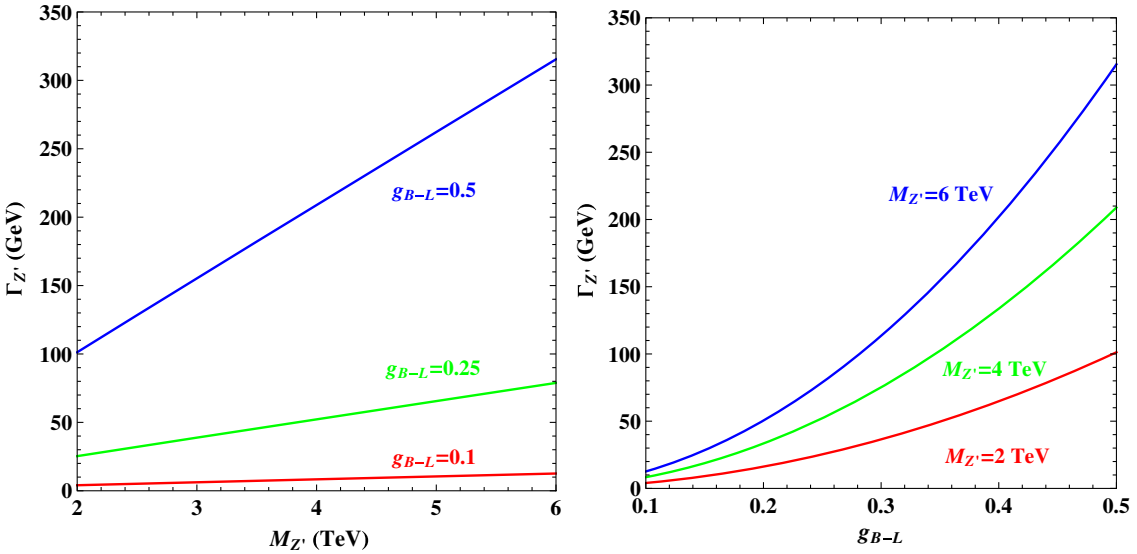

FIG. 6 (color online). Total decay width of Z' as a function of $M_{Z'}$ (for fixed values of g_{B-L}), and g_{B-L} (for fixed values of $M_{Z'}$).

The branching ratios of H decaying into other new physical particles are below 10^{-3} in this case, while for $M_H \gg M_W$, it is well known that decays of H into vector bosons are determined by their Goldstone nature, which implies

$$\mathrm{BR}(H \to hh) \approx \mathrm{BR}(H \to ZZ) \approx \frac{1}{2}\mathrm{BR}(H \to WW). \quad (30)$$

The asymptotic behavior of this relation is clearly shown in the left panel of Fig. 5. On the other hand, for a relatively small mixing angle $\sin\theta = 0.01$, decays of H into SM particles will be suppressed and decays into new particles will be greatly enhanced. $H \to SS^*$ is dominant when $M_H < 400$ GeV. The branching ratio of $\psi\bar{\psi}$ will reach about 0.25 when $M_H \sim 600$ GeV, which is comparable with $H \to W^+W^-$. In this case, $H \to F\bar{F}$ is below 10% and $H \to \eta^+\eta^-/A_1^0A_1^{0*}$ is below 2%.

The heavy neutral Higgs H is testable for a large mixing angle θ. For example, the promising channels to probe the heavy neutral Higgs H would be $ZZ \to 4l$, $ZZ \to 2l2\nu$, $ZZ \to 2l2j$, $ZZ \to 2l2\tau$, $WW \to 2l2\nu$, $WW \to l\nu 2j$, $hh \to 4b$, and $hh \to 2b2\gamma$ [56]. At the same time, we would like to mention that the heavy Higgs H could enhance the di-Higgs production hh [57] by a factor of 18 compared to the standard model case [58]. For a small mixing angle θ, the production of H will be suppressed by this small θ, thus making it challenging to probe directly at colliders.

TABLE II. Branching ratios of Z' at our benchmark point. Here, we set $M_H = 300$ GeV and $\sin\theta = 0$ for simplicity.

$q\bar{q}$	$l\bar{l}$	$\nu_L\bar{\nu}_L$	$\psi\bar{\psi}$	$N_{R1}\bar{N}_{R1}$	$N_{R2}\bar{N}_{R2}$	$\chi_1\bar{\chi}_1$	$\chi_2\bar{\chi}_2$
0.25	0.38	0.19	0.063	0.0077	0.0077	0.016	0.032
HH	hh	$A_1^0A_1^{0*}$	$H_1^0H_1^{0*}$	$A_2^0A_2^{0*}$	$H_2^0H_2^{0*}$	$\eta_1^+\eta_1^-$	$\eta_2^+\eta_2^-$
0.030	0	0.0076	0.0051	0.0010	0.0013	0.0076	0.0010

Next we review the properties of the $U(1)_{B-L}$ gauge boson Z'. With about 20 fb^{-1} of data at the 8 TeV LHC, the bound on Z' has been pushed up to 2.95 TeV by CMS through the ratio $R_\sigma = \sigma(pp \to Z' \to \ell^+\ell^-)/\sigma(pp \to Z \to \ell^+\ell^-)$, where $\ell = e, \mu$ [59]. At our benchmark point, we choose $M_{Z'} = 4$ TeV and $g_{B-L} = 0.5$ ($v_\sigma = 8$ TeV), which can safely satisfy current experimental limits and can be tested at *the* 14 TeV LHC with 100 fb^{-1} [60,61]. Figure 6 shows the total decay width of Z' as a function of $M_{Z'}$ and g_{B-L}. Depending on g_{B-L}, $\Gamma_{Z'}$ varies from a few to hundreds of GeV. If $\Gamma_{Z'}$ is this large, it can be directly measured by the leptonic final states at the LHC [60,61].

In Table II, the decay branching ratios of Z' are presented under the benchmark point. The dominant decay channels are $q\bar{q}$, $l\bar{l}$, and $\nu_L\bar{\nu}_L$, while all of the new particle final states only account for about 20%. A distinct feature of the $U(1)_{B-L}$ gauge boson Z' is the definite relation between the quark and lepton final states:

$$\mathrm{BR}(Z' \to q\bar{q}) : \mathrm{BR}(Z' \to l\bar{l}) \simeq 2:3 \quad (31)$$

after summing over all flavors. This relation can be used to distinguish the $U(1)_{B-L}$ gauge boson Z' from Z' in other models [20]. More practically, in experiments the $B-L$ nature of Z' can be tested if $\mathrm{BR}(Z' \to b\bar{b})/\mathrm{BR}(Z' \to \mu^+\mu^-) = 1/3$ is confirmed [13]. In our model with only left-handed light neutrinos, the dominant invisible decay channel of Z' is $\mathrm{BR}(Z' \to \nu_L\bar{\nu}_L)$, which is half of $\mathrm{BR}(Z' \to l\bar{l})$. Further with the dark matter candidate in our model, Z' invisible decays get additional contributions from Z' into dark matter pairs. For instance, $\mathrm{BR}(Z' \to \mathrm{inv})$ could be 0.2457, 0.1990, 0.1964 for FF, FS and SS dark

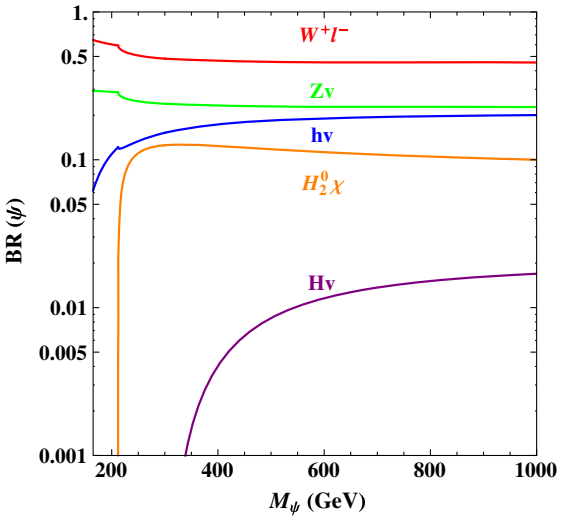

FIG. 7 (color online). Branching ratios of ψ as a function of M_ψ. We have fixed $\sin\theta = 0.3$, $M_H = 300$ GeV and $y = h = 2.8 \times 10^{-3}$.

matter respectively. So a precise measurement of BR($Z' \to$ inv) would shed light on the nature of dark matter.

Another interesting feature of our model is the existence of the heavy Dirac fermion ψ; thus there are no lepton-number-violation (LNV) decays as $\psi \to W^- l^+$. For $M_\psi < M_h$, the Higgs decay into a pair of light and heavy neutrinos, $h \to \bar{\nu}\psi + \bar{\psi}\nu$ will open, which could increase Γ_h by up to almost 30% and significantly affect Higgs searches at the LHC [62]. In this paper, we consider $M_\psi > M_h$. Therefore, the decay channels of ψ could be W^+l^-, $Z\nu$, $h\nu$, and if kinematically allowed $H\nu$, $A_i^0 N_j$, $A_i^0\chi_j$, $H_i^0 N_j$, $H_i^0\chi_j (i,j = 1,2)$ are also possible. Due to the tiny mixing angle $\theta_{1,2}$, the branching ratios of $\psi \to A_i^0 N_j$, $A_i^0\chi_j$ are negligible. In Fig. 7, we show the branching ratios of ψ. It is clear that ψ will decay predominantly into standard model final states for comparable Yukawa couplings of y and h. Approximately for $M_\psi \gg M_W$, we have

$$\frac{1}{\cos^2\theta}\mathrm{BR}(\psi \to h\nu) \approx \mathrm{BR}(\psi \to Z\nu) \approx \frac{1}{2}\mathrm{BR}(\psi \to W^+l^-). \tag{32}$$

Decays of ψ into new physical particles are small in this case. BR($\psi \to H_2^0\chi$) is about 10%, once it is kinematically opened. BR($\psi \to H\nu$) is suppressed by $\sin^2\theta$, and thus it is always much smaller. As shown in Table II, BR($Z' \to \psi\bar{\psi}$) $\simeq 0.063$ for one generation in our model, so $\psi\bar{\psi}$ can be produced through the Z' portal. A possible promising signature is the trilepton channel [60]:

$$pp \to Z' \to \psi\bar{\psi} \to W^+l^- + W^-l^+ \to 2l^\pm l^\mp jj + \not{E}_T. \tag{33}$$

TABLE III. Production cross sections for inert scalar doublets.

Particles	$\eta_1^+\eta_1^-$	$\eta_1^\pm A_1^0$	$A_1^0 A_1^{0*}$	$\eta_2^+\eta_2^-$	$\eta_2^\pm A_2^0$	$A_2^0 A_2^{0*}$
σ (in fb)	5.8	16	3.6	0.089	0.31	0.075

The cross section of this trilepton signal is about 0.017 fb at our benchmark point, so the trilepton is only promising at the future high-luminosity LHC. The mass of ψ can be reconstructed using the transverse mass of two opposite-sign leptons with missing transverse momentum [60]. Another feature of ψ is the possible large mixing with ν_L compared to the canonical type-I seesaw [3]. As discussed in Sec. II C, the mixing $V_{\nu\psi}$ between ν_L and ψ_L is $M_D/\sqrt{M_D^2 + M_\psi^2}$. For $M_D \sim \mathcal{O}(1)$ GeV, $M_\psi \sim \mathcal{O}(100)$ GeV, $V_{\nu\psi} \sim \mathcal{O}(10^{-2})$. Therefore, ψ could be largely associated produced with charged leptons through W [63]:

$$pp \to W^* \to l^\pm\psi \to l^\pm + W^\pm l^\mp \to l^\pm l^\mp jj, \tag{34}$$

$$pp \to W^* \to l^\pm\psi \to l^\pm + W^\pm l^\mp \to l^\pm l^\mp l^\pm \not{E}_T. \tag{35}$$

The production cross section $\sigma(l^\pm\psi) = 350 \times |V_{i\psi}|^2$ fb at our benchmark point. And it might be promising at the 14 TeV LHC with about 100 fb^{-1}. The testability of this heavy Dirac neutrino ψ is less promising than the heavy Majorana neutrinos with the same mixing scale, since the latter could give rise to LNV signatures [64–67].

Finally, we discuss the decays of inert scalars and fermions. N_{R1} and H_2^0 are dark matter candidates at our benchmark point in Eq. (22). Decays of N_{R2} are dominated by $N_{R2} \to l^\pm\eta_1^{\mp *} \to l^\pm l^\mp N_{R1}$ and $N_{R2} \to \nu A_1^{0*} \to \nu\nu N_{R1}$ through the Yukawa coupling f. Decays of χ_i are $\chi_i \to H_2^0\psi^*$ with the off-shell ψ^* further decaying into $W^+l^-/Z\nu/h\nu/H_2^0\nu.A_1^0$ and $\eta_1^\pm$ mainly decay through the Yukawa coupling f, which leads to $A_1^0 \to \nu N_{Ri}$ and $\eta_1^\pm \to l^\pm N_{Ri}$. The heavy Z_2 odd scalar H_1^0 decays into ψN_{Ri} through the Yukawa coupling h_α and into hA_1^0 through the trilinear coupling μ_1. Similarly, decays of A_2^0 are $A_2^0 \to \nu\chi_i$ and $A_2^0 \to hH_2^0$, while decays of $\eta_2^\pm$ are $\eta_2^\pm \to l^\pm\chi_i$ and $\eta_2^\pm \to W^\pm H_2^0$.

The inert scalar doublets can be pair produced through the Drell-Yang process. In Table III, we list the production cross sections for inert scalar doublets. Many signatures can arise from the inert particles. In Ma's scotogenic model [9], promising signals of the doublet scalar at colliders are multilepton final states with missing transverse energy $\not{E}_T$ [68–70]. Similar signals can also be produced in our model, for example

$$2l + \not{E}_T:\ \eta_1^+\eta_1^- \to l^+ N_{R1} + l^- N_{R1},$$
$$:\ \eta_2^+\eta_2^- \to W^+ H_2^{0*} + W^- H_2^0 \to l^+\nu_l H_2^{0*} + l^-\bar{\nu}_l H_2^0, \quad (36)$$

$$3l + \not{E}_T:\ \eta_1^+ A_1^0 \to l^+ N_{R2} + \nu N_{R1} \to l^+ l^\pm l^\mp N_{R1} + \nu N_{R1},$$
$$:\ \eta_2^\pm A_2^0 \to W^\pm H_2^{0(*)} + hH_2^0 \to l^\pm \nu_l H_2^{0(*)} + l^+\nu_l l^-\bar{\nu}_l H_2^0, \quad (37)$$

$$4l + \not{E}_T:\ \eta_1^+\eta_1^- \to l^+ N_{R2} + l^- N_{R1} \to l^+ l^\pm l^\mp N_{R1} + l^- N_{R1},$$
$$:\ A_2^0 H_2^{0*} \to hH_2^0 H_2^{0*} \to l^+ l^- l^+ l^- H_2^0 + H_2^{0*}. \quad (38)$$

With such different decay topologies between Ma's model and ours, it would be distinguishable even with the same signals. Apart from these multilepton signals, there are also some other interesting signals in our model, i.e.

$$2l^\pm jj + \not{E}_T:\ \eta_2^\pm A_2^0 \to W^\pm H_2^{0(*)} + hH_2^0 \to l^\pm \nu_l H_2^{0(*)} + l^\pm \nu_l jj H_2^0, \quad (39)$$

$$l^\pm b\bar{b} + \not{E}_T:\ \eta_2^\pm A_2^0 \to W^\pm H_2^{0(*)} + hH_2^0 \to l^\pm \nu_l H_2^{0(*)} + b\bar{b}H_2^0. \quad (40)$$

The lepton-number-violation signal $2l^\pm jj + \not{E}_T$ suffers a much lower SM background, which might make this signal very promising at the LHC. The $l^\pm b\bar{b} + \not{E}_T$ has a relatively large production rate due to the fact that $h \to b\bar{b}$ is dominant in h decay, so it might also be promising.

IV. CONCLUSIONS

The usual canonical seesaw mechanisms require the heavy states to have a mass scale at the grand unification scale in order to generate the small neutrino mass. In the linear seesaw scenario with $m_\nu \simeq \mu_L M_D/M_\Psi$, the neutrino masses suffer a twofold suppression by both the lepton number symmetry-violating term μ_L and the heavy mass M_Ψ. The linear seesaw model can lower the seesaw scale such that new physics may arise at the TeV scale. In this work, we constructed a radiated linear seesaw model where the naturally small term μ_L was generated at the one-loop level and its soft breaking of lepton number symmetry contributes to the SSB of $B-L$ symmetry at the TeV scale. To satisfy the cancellation of anomalies, the value of $B-L$ charges for inert particles are found to be exotic such that there exists a residual $Z_2 \times Z_2'$ symmetry even after SSB of the $B-L$ gauge symmetry. It was shown that the residual symmetry stabilizes the inert particles as dark matter candidates. In our model, we introduced two classes of inert particles to realize the model such that the lightest inert particles in each class play the role of the dark matter candidate. Therefore we have proposed a two-component dark matter model. The seesaw scale of the radiated linear seesaw scale can be as low as a few hundred GeV, leading to interesting phenomenology.

Given the benchmark point, the main phenomenological predictions were illustrated. For the Yukawa coupling $f_{li}(f_l)$ at 0.01 order and $\eta_1(\eta_2)$ with mass 270 GeV (690 GeV), it predicts $\mathrm{Br}(\mu \to e\gamma) \sim 10^{-13}$, an order slightly under the current constraints and in the reach of forthcoming experiments. The two-component dark matter candidates are realized in our model. To account for the observed relic density, the annihilation of dark matter is dominated by the s-channel scalars h/H or the gauge boson Z'. For the fermion dark matter, we found that the h channel is excluded. But it is still allowed for the H channel and the Z' channel. On the contrary, for the scalar DM, the Z' channel is excluded while the h/H channel is allowed. And the heavy Higgs H also plays a vital role in the conversion between fermion and scalar dark matter. Collider signatures of our model are also very rich. The precise measurements of the SM Higgs h will put a tight constraint on light scalar DM and heavy scalar H. With a relatively large mixing angle $\sin\theta = 0.3$, the $H \to ZZ$, W^+W^-, channels are testable at the LHC. For the extra Z boson and heavy lepton ψ, the trilepton channel of $Z \to \bar{\psi}\psi$ is promising at the HL-LHC. With a larger cross section, the associated production of $l^\pm\psi$ may be more promising. The inert doublet scalar can also produce multilepton channels. And some distinct channels, such as $2\ell^\pm jj + \not{E}_T$, $\ell^\pm bb + \not{E}_T$, can be used to distinguish our model.

Finally, we would like to mention that the radiated linear seesaw model we proposed is the minimal version where only one Ψ fermion mediator is included. In this scenario, M_ν is a rank-2 mass matrix and the lightest neutrino must be massless. However, more complicated scenarios exist, corresponding to other solutions of the anomaly free condition. Then one may obtain the rank-3 neutrino mass matrix. Such scenarios predict more new particles with different $B-L$ charges, and thus the model construction and the phenomenology deserve further study.

ACKNOWLEDGMENTS

We would like to thank Ran Ding for help with the analysis of dark matter. The work of W. W. is supported by National Natural Science Foundation of China under Grant No. 11505062, Special Fund of Theoretical Physics under Grant No. 11447117 and Fundamental Research Funds for the Central Universities

[1] Q. R. Ahmad *et al.* (SNO Collaboration), Phys. Rev. Lett. **89**, 011301 (2002); K. Eguchi *et al.* (KamLAND Collaboration), Phys. Rev. Lett. **90**, 021802 (2003); M. H. Ahn *et al.* (K2K Collaboration), Phys. Rev. Lett. **90**, 041801 (2003); F. P. An *et al.* (DAYA-BAY Collaboration), Phys. Rev. Lett. **108**, 171803 (2012); J. K. Ahn *et al.* (RENO Collaboration), Phys. Rev. Lett. **108**, 191802 (2012).

[2] S. Weinberg, Phys. Rev. Lett. **43**, 1566 (1979).

[3] P. Minkowski, Phys. Lett. B **67**, 421 (1977); T. Yanagida, in *Proceedings of the Workshop on Unified Theories and Baryon Number in the Universe*, edited by O. Sawada *et al.* (KEK Report 79-18, Tsukuba, 1979), p. 95; M. Gell-Mann, P. Ramond, and R. Slansky, in *Supergravity*, edited by P. Van Niewenhuizen*et al.* (North-Holland, Amsterdam, 1979), p. 315; S. Glashow, in *Quarks and Leptons*, edited by M. Lévy *et al.* (Plenum, New York, 1980), p. 707; R. N. Mohapatra and G. Senjanović, Phys. Rev. Lett. **44**, 912 (1980).

[4] R. N. Mohapatra and G. Senjanović, Phys. Rev. Lett. **44**, 912 (1980); J. Schechter and J. W. F. Valle, Phys. Rev. D **22**, 2227 (1980); **25**, 774 (1982).

[5] D. Weyler and L. Wolfenstein, Nucl. Phys. **B218**, 205 (1983); R. N. Mohapatra and J. W. F. Valle, Phys. Rev. D **34**, 1642 (1986); E. Ma, Phys. Lett. B **191**, 287 (1987).

[6] E. Akhmedov, M. Lindner, E. Schnapka, and J. W. F. Valle, Phys. Lett. B **368**, 270 (1996); Phys. Rev. D **53**, 2752 (1996).

[7] M. Malinsky, J. C. Romao, and J. W. F. Valle, Phys. Rev. Lett. **95**, 161801 (2005).

[8] A. Zee, Phys. Lett. B **93**, 389 (1980); A. Pilaftsis, Z. Phys. C **55**, 275 (1992).

[9] E. Ma, Phys. Rev. D **73**, 077301 (2006).

[10] J. Kubo, E. Ma, and D. Suematsu, Phys. Lett. B **642**, 18 (2006); P. H. Gu and U. Sarkar, Phys. Rev. D **77**, 105031 (2008); E. Ma and D. Suematsu, Mod. Phys. Lett. A **24**, 583 (2009); D. Aristizabal Sierra, J. Kubo, D. Suematsu, D. Restrepo, and O. Zapata, Phys. Rev. D **79**, 013011 (2009); S. Kanemura, T. Nabeshima, and H. Sugiyama, Phys. Lett. B **703**, 66 (2011); S. Kanemura, O. Seto, and T. Shimomura, Phys. Rev. D **84**, 016004 (2011); S. Kanemura and H. Sugiyama, Phys. Rev. D **86**, 073006 (2012); H. Okada and T. Toma, Phys. Rev. D **86**, 033011 (2012); P. S. Bhupal Dev and A. Pilaftsis, Phys. Rev. D **86**, 035002 (2012); D. Schmidt, T. Schwetz, and T. Toma, Phys. Rev. D **85**, 073009 (2012); M. Hirsch, R. A. Lineros, S. Morisi, J. Palacio, N. Rojas, and J. W. F. Valle, J. High Energy Phys. 10 (2013) 149; D. Restrepo, O. Zapata, and C. E. Yaguna, J. High Energy Phys. 11 (2013) 011; S. S. Law and K. L. McDonald, J. High Energy Phys. 09 (2013) 092; S. Kanemura, T. Matsui, and H. Sugiyama, Phys. Lett. B **727**, 151 (2013); V. Brdar, I. Picek, and B. Radovcic, Phys. Lett. B **728**, 198 (2014); H. Okada and K. Yagyu, Phys. Rev. D **90**, 035019 (2014); H. Okada, N. Okada, and Y. Orikasa, arXiv:1504.01204; S. Baek, H. Okada, and K. Yagyu, J. High Energy Phys. 04 (2015) 049.

[11] A. Zee, Nucl. Phys. **B264**, 99 (1986); K. S. Babu, Phys. Lett. B **203**, 132 (1988).

[12] E. Ma, Phys. Lett. B **662**, 49 (2008).

[13] S. Kanemura, T. Nabeshima, and H. Sugiyama, Phys. Rev. D **85**, 033004 (2012).

[14] S. Kanemura, T. Matsui, and H. Sugiyama, Phys. Rev. D **90**, 013001 (2014).

[15] G. Gang, X. G. He, and G. N. Li, J. High Energy Phys. 10 (2012) 044; Y. Kajiyama, H. Okada, and T. Toma, Phys. Rev. D **88**, 015029 (2013); Y. Kajiyama, H. Okada, and K. Yagyu, Nucl. Phys. **B874**, 198 (2013); G. N. Li, G. Gang, B. Ren, Y. J. Zheng, and X. G. He, J. High Energy Phys. 04 (2013) 026; M. Aoki and T. Toma, J. Cosmol. Astropart. Phys. 09 (2014) 016; H. Okada, T. Toma, and K. Yagyu, Phys. Rev. D **90**, 095005 (2014); S. Baek, H. Okada, and T. Toma, J. Cosmol. Astropart. Phys. 06 (2014) 027; S. Kashiwase, H. Okada, Y. Orikasa, and T. Toma, arXiv: 1505.04665; C. Q. Geng, D. Huang, L. H. Tsai, and Q. Wang, J. High Energy Phys. 08 (2015) 141.

[16] L. M. Krauss, S. Nasri, and M. Trodden, Phys. Rev. D **67**, 085002 (2003); K. Cheung and O. Seto, Phys. Rev. D **69**, 113009 (2004); M. Aoki, S. Kanemura, and O. Seto, Phys. Rev. Lett. **102**, 051805 (2009); M. Gustafsson, J. M. No, and M. A. Rivera, Phys. Rev. Lett. **110**, 211802 (2013); J. N. Ng and A. de la Puente, Phys. Lett. B **727**, 204 (2013); A. Ahriche, C.-S. Chen, K. L. McDonald, and S. Nasri, Phys. Rev. D **90**, 015024 (2014); C.-S. Chen, K. L. McDonald, and S. Nasri, Phys. Lett. B **734**, 388 (2014); C. Q. Geng, D. Huang, and L. H. Tsai, Phys. Rev. D **90**, 113005 (2014); H. Okada and Y. Orikasa, Phys. Rev. D **90**, 075023 (2014); H. Hatanaka, K. Nishiwaki, H. Okada, and Y. Orikasa, Nucl. Phys. **B894**, 268 (2015); K. Nishiwaki, H. Okada, and Y. Orikasa, arXiv:1507.02412 [Phys. Rev. D (to be published)]; L. G. Jin, R. Tang, and F. Zhang, Phys. Lett. B **741**, 163 (2015); C. Q. Geng, D. Huang, and L. H. Tsai, Phys. Lett. B **745**, 56 (2015).

[17] F. Bonnet, M. Hirsch, T. Ota, and W. Winter, J. High Energy Phys. 07 (2012) 153.

[18] E. Ma, Mod. Phys. Lett. A **17**, 535 (2002).

[19] S. Khalil, J. Phys. G **35**, 055001 (2008).

[20] P. Langacker, Rev. Mod. Phys. **81**, 1199 (2009).

[21] G. Cacciapaglia, C. Csaki, G. Marandella, and A. Strumia, Phys. Rev. D **74**, 033011 (2006).

[22] G. Aad *et al.* (ATLAS Collaboration), Phys. Lett. B **716**, 1 (2012).

[23] S. Chatrchyan *et al.* (CMS Collaboration), Phys. Lett. B **716**, 30 (2012).

[24] V. Barger, P. Langacker, and G. Shaughnessy, Phys. Rev. D **75**, 055013 (2007).

[25] V. Barger, P. Langacker, M. McCaskey, M. J. Ramsey-Musolf, and G. Shaughnessy, Phys. Rev. D **77**, 035005 (2008).

[26] T. Robens and T. Stefaniak, Eur. Phys. J. C **75**, 104 (2015).

[27] H. Fritzsch and Z. Z. Xing, Phys. Lett. B **372**, 265 (1996); **413**, 396 (1997); **440**, 313 (1998); Y. Koide, Mod. Phys. Lett. A **11**, 2849 (1996); Y. Koide and S. Fusaoka, Prog. Theor. Phys. **97**, 459 (1997); Z. Z. Xing, D. Yang, and S. Zhou, Phys. Lett. B **690**, 304 (2010); S. Dev, S. Gupta, and R. R. Gautam, Phys. Lett. B **702**, 28 (2011).

[28] S. K. Garg and S. Gupta, J. High Energy Phys. 10 (2013) 128.

[29] D. S. Akerib *et al.* (LUX Collaboration), Phys. Rev. Lett. **112**, 091303 (2014).

[30] T. Toma and A. Vicente, J. High Energy Phys. 01 (2014) 160.

[31] A. Vicente and C. E. Yaguna, J. High Energy Phys. 02 (2015) 144
[32] J. Adam *et al.* (MEG Collaboration), Phys. Rev. Lett. **110**, 201801 (2013).
[33] J. Hisano, T. Moroi, K. Tobe, and M. Yamaguchi, Phys. Rev. D **53**, 2442 (1996).
[34] A. M. Baldini *et al.*, arXiv:1301.7225.
[35] B. Aubert *et al.* (*BABAR* Collaboration), Phys. Rev. Lett. **104**, 021802 (2010).
[36] K. Hayasaka *et al.*, Phys. Lett. B **687**, 139 (2010).
[37] P. A. R. Ade *et al.* (Planck Collaboration), Astron. Astrophys. **571**, A16 (2014).
[38] G. Bertone, D. Hooper, and J. Silk, Phys. Rep. **405**, 279 (2005).
[39] N. D. Christensen and C. Duhr, Comput. Phys. Commun. **180**, 1614 (2009); A. Alloul, N. D. Christensen, C. Degrande, C. Duhr, and B. Fuks, Comput. Phys. Commun. **185**, 2250 (2014).
[40] G. Blanger, F. Boudjema, A. Pukhov, and A. Semenov, Comput. Phys. Commun. **192**, 322 (2015); **185**, 960 (2014); **176**, 367 (2007).
[41] S. Esch, M. Klasen, and C. E. Yaguna, J. High Energy Phys. 09 (2014) 108.
[42] Q. H. Cao, E. Ma, J. Wudka, and C.-P. Yuan, arXiv: 0711.3881.
[43] M. Aoki, M. Duerr, J. Kubo, and H. Takano, Phys. Rev. D **86**, 076015 (2012).
[44] G. Aad *et al.* (ATLAS and CMS Collaborations), Phys. Rev. Lett. **114**, 191803 (2015).
[45] A. Arhrib, R. Benbrik, and N. Gaur, Phys. Rev. D **85**, 095021 (2012).
[46] S. Baek, P. Ko, and W. I. Park, Phys. Rev. D **90**, 055014 (2014).
[47] G. Aad *et al.* (ATLAS Collaboration), Phys. Rev. Lett. **112**, 201802 (2014).
[48] P. Bechtle, S. Heinemeyer, O. Stål, T. Stefaniak, and G. Weiglein, J. High Energy Phys. 11 (2014) 039.
[49] T. Corbett, O. J. P. Eboli, D. Goncalves, J. Gonzalez-Fraile, T. Plehn, and M. Rauch, J. High Energy Phys. 08 (2015) 156.
[50] G. Aad *et al.* (ATLAS Collaboration), arXiv:1507.04548.
[51] C. Bernaciak, T. Plehn, P. Schichtel, and J. Tattersall, Phys. Rev. D **91**, 035024 (2015).
[52] P. P. Giardino, K. Kannike, I. Masina, M. Raidal, and A. Strumia, J. High Energy Phys. 05 (2014) 046.
[53] A. Falkowski, F. Riva, and A. Urbano, J. High Energy Phys. 11 (2013) 111.
[54] M. Pelliccioni (CMS Collaboration), arXiv:1505.03831.
[55] S. Dawson *et al.*, arXiv:1310.8361.
[56] D. Buttazzo, F. Sala, and A. Tesi, arXiv:1505.05488.
[57] J. Baglio, A. Djouadi, R. Gröber, M. M. Mhlleitner, J. Quevillon, and M. Spira, J. High Energy Phys. 04 (2013) 151.
[58] C. Y. Chen, S. Dawson, and I. M. Lewis, Phys. Rev. D **91**, 035015 (2015).
[59] V. Khachatryan *et al.* (CMS Collaboration), J. High Energy Phys. 04 (2015) 025.
[60] L. Basso, A. Belyaev, S. Moretti, and C. H. Shepherd-Themistocleous, Phys. Rev. D **80**, 055030 (2009).
[61] L. Basso, A. Belyaev, S. Moretti, G. M. Pruna, and C. H. Shepherd-Themistocleous, Eur. Phys. J. C **71**, 1613 (2011).
[62] J. H. Chen, X. G. He, J. Tandean, and L. H. Tsai, Phys. Rev. D **81**, 113004 (2010).
[63] G. Bambhaniya, S. Goswami, S. Khan, P. Konar, and T. Mondal, Phys. Rev. D **91**, 075007 (2015).
[64] T. Han and B. Zhang, Phys. Rev. Lett. **97**, 171804 (2006).
[65] F. del Aguila, J. A. Aguilar-Saavedra, and R. Pittau, J. High Energy Phys. 10 (2007) 047.
[66] A. Atre, T. Han, S. Pascoli, and B. Zhang, J. High Energy Phys. 05 (2009) 030.
[67] F. F. Deppisch, P. S. B. Dev, and A. Pilaftsis, New J. Phys. **17**, 075019 (2015).
[68] E. Dolle, X. Miao, S. Su, and B. Thomas, Phys. Rev. D **81**, 035003 (2010).
[69] X. Miao, S. Su, and B. Thomas, Phys. Rev. D **82**, 035009 (2010).
[70] M. Gustafsson, S. Rydbeck, L. Lopez-Honorez, and E. Lundstrom, Phys. Rev. D **86**, 075019 (2012).